Plant Gene 28 (2021) 100344

Contents lists available at ScienceDirect

Plant Gene

journal homepage: www.elsevier.com/locate/plantgene

Genome-wide exploration of auxin response factors (ARFs) and their expression dynamics in response to abiotic stresses and growth regulators in coconut (*Cocos nucifera* L.)

Santhi C.K.V. [a,1], Rajesh M.K. [a,*,1], Ramesh S.V. [a], Muralikrishna K.S. [a], Gangaraj K.P. [a], Gupta Payal [b], Dash Prasanta K. [b,*]

[a] *ICAR-Central Plantation Crops Research Institute, Kasaragod 671124, Kerala, India*
[b] *ICAR-National Institute for Plant Biotechnology, Pusa Campus, New Delhi 110012, India*

ARTICLE INFO

Keywords:
Coconut
ARF
Gene expression pattern
Abiotic stress
Protein–protein interaction

ABSTRACT

Auxin response factors (ARFs) are a class of transcription factors with the ability to bind specifically to the promoter region of auxin-responsive genes in plants and thereby modulate various aspects of biological processes and responses to diverse environmental conditions. Identification and characterization of ARF gene families have been undertaken in various plant species; however, no such data, delineating *ARF*s in coconut, is available. Through genome-wide analysis, we have identified 20 *CnARF* (*Cocos nucifera ARF*) genes in the genome of a dwarf cultivar, Chowghat Green Dwarf. Evolutionary analysis of *CnARF*s, along with *ARF*s from oil palm and date palm, showed that palm *ARF*s could be classified into three major clades. Multiple sequence alignment and analysis of conserved motifs revealed that majority of the CnARFs harbored all the three principal domains (i.e. N-terminus DNA binding domain, an ARF sub-domain and an AUX/IAA sub-domain), which are characteristic of all plant ARFs. Quantitative real-time PCR-based expression analysis of ARFs of mature zygotic embryos, exposed to osmotic and temperature stresses and growth regulators, suggest a complex and stress-specific transcriptional response of coconut embryo-derived *ARF*s. Collectively, these findings offer valuable information and the first molecular insights into the *CnARF*s, laying the foundation for further functional characterization in developmental and reproductive pathways and their inclusion in breeding for stress tolerance in coconut.

1. Introduction

The phytohormone auxin regulates various growth and developmental processes in plants, including morphogenesis, phototropism, responses to extreme environments (such as cold, water stress and salinity), floral opening, development of seeds and dormancy, and plant-microbe interactions (Matilla, 2020; Wu et al., 2020; Kunkel and Johnson, 2021). Myriads of experimental evidence have shown this regulation is achieved by the modulation of expression of various genes. *Aux/IAA* (*Indole-3-acetic acid-inducible gene*), *GH3* (*Gretchen Hagen 3*), *SAUR* (*small auxin up RNA)* (Hagen and Guilfoyle, 2002), *YUC* (*YUCCA*) and *PIN* (*PIN-FORMED*) (Feher, 2015) are some of the gene families that are modulated in response to auxin treatment. Many of these early responsive genes are characterized, in their promoter region, with one or more copies of the canonical motifs ('TGTCGG' or 'TGTCTC') known as auxin-responsive element (AuxRE) (Roosjen et al., 2018). Interaction of transcription factors (TFs) with AuxRE has been the hallmark of the auxin signaling pathway. One such family of TFs is the Auxin Response Factor (ARF), which modulates the expression patterns of auxin-responsive genes by specifically binding with the AuxRE (Liscum and Reed, 2002; Guilfoyle and Hagen, 2007). Progress in the field of auxin biology has highlighted the role of three major domains in the ARF protein family: (i) a N-terminus DNA-binding domain (DBD), which belongs to B3 like family; (ii) a variable transcriptional regulator in the middle region (MR), followed by (iii) a C-terminus PB1 domain (previously known as domain III/IV) (reviewed in Weijers and Wagner, 2016). The N-terminal B3 type DBD, which is highly conserved, specifically recognizes and binds to the ARF-specific AuxRE (Boer et al., 2014). The

Abbreviations: ARF, auxin response factors; TF, transcription factors; CGD, Chowghat Green Dwarf; IAA, indole acetic acid; MR, middle region.

* Corresponding authors.
E-mail addresses: rajesh.mk@icar.gov.in (R. M.K.), prasanta01@yahoo.com (D. Prasanta K.).

[1] These authors contributed equally to this manuscript.

https://doi.org/10.1016/j.plgene.2021.100344
Received 1 October 2020; Received in revised form 9 September 2021; Accepted 7 October 2021
Available online 31 October 2021

variable MR region, on the other hand, possesses the ability to either repress or activate transcription from promoters which contain the conserved AuxRE; the ability to activate or repress is decided by the abundance of certain amino acid in the MR (Tiwari et al., 2003). While an enrichment of glutamines in the MR makes it to function as an activator (ARFs of class A), an abundance of serines, prolines, and threonines results in the MR functioning as a repressor (ARFs of classes B and C) (Tiwari et al., 2003). The CTD domain participates in protein-protein interactions by permitting ARF homo-dimerization and ARF- Aux/IAA hetero-dimerization (Pérez-Rodríguez et al., 2010; Zhang et al., 2011).

Detailed studies of the auxin signaling pathway have revealed that at low levels of auxin, members of Aux/IAA protein family form dimers with ARFs (of class A), causing the target genes to be repressed with the help of TOPLESS (TPL) and via histone deacetylase recruitment (Szemenyei et al., 2008). In contrast, at elevated levels of auxin, Aux/IAA proteins are recognized by SKP1-Cullin-F-Box protein complex comprising of the transport inhibitor response 1 protein (SCF^{TIR1}) auxin receptor or auxin signaling F-box protein (AFB) family members and hastens the Aux/IAA protein degradation by the 26S proteasome. The ARFs that become free ultimately regulate the transcription of their target genes (Kepinski and Leyser, 2005; Dharmasiri et al., 2005). Therefore, while class A ARFs mainly mediate auxin responses, class B and C ARFs, in contrast, do not display strong binding to Aux/IAA proteins and can repress gene expression by themselves (Chandler, 2016).

The genome-wide expression profiling of *ARF*s has been undertaken in various plant species. These studies have revealed the presence of 23 members in *Arabidopsis* (Okushima et al., 2005), 25 in *Oryza sativa* (Wang et al., 2007), 31 in *Zea mays* (Xing et al., 2011), 20 in *Hordeum vulgare* (Tombuloglu, 2019), 20 in *Solanum tuberosum* (Song et al., 2019) and 52 ARFs in *Triticum aestivum* (Gidhi et al., 2020).

The specific roles of individual ARFs in plant development have been documented utilizing several loss-of-function ARF mutants. For instance, in *Arabidopsis thaliana, Atarf3* displayed defective patterning of the carpels (Nishimura et al., 2005); *Atarf5* exhibited abnormal vascular strands, embryonic axis and root development (Hardtke and Berleth, 1998); *Atarf7* mutants have impaired gravitropic, phototropic responses and weak hypocotyl response to auxin stimulus (Harper et al., 2000); *Atarf8* mutants showed long hypocotyl and affected auxin equillibrium (Goetz et al., 2006); *Atarf7/Atarf19* double mutant has been shown to have affected the growth of lateral root (Narise et al., 2010) and *Atarf6/Atarf8* double mutants show impairment in maturation of flowers (Nagpal et al., 2005).

Recent advances in the perception of the ARFs have enabled the exploration of its role and expression pattern in various plant species. For instance, in rice, *ARF12* is involved in Fe equilibrium (Qi et al., 2012), while *ARF16* regulates the uptake of PO_4^{3-} ions. Moreover, the unusual morphological change displayed by transgenic rice expressing antisense *ARF1* has revealed its significance in various growth and developmental stage of rice plant (Aya et al., 2014). Above all, growing bodies of evidence implicate the role of ARF gene family as a "molecular defender" against biotic or abiotic stresses and the adversity of the condition determines whether it should act as either a positive or as a negative modulator (Li et al., 2016).

Coconut (*Cocos nucifera* L.; Arecaceae) is an important palm covering an approximate area of around 11.81 million ha in the tropical and subtropical regions, with 62.46 million nuts produced annually (FAO, 2021). A repertoire of studies on the transcriptional and post-transcriptional regulation during zygotic embryogenesis (Bandupriya and Dunwell, 2015), somatic embryogenesis (Rajesh et al., 2016; Sabana et al., 2020) and disease progression (Nejat et al., 2015; Rajesh et al., 2015, 2018; Gangaraj and Rajesh, 2020) have been undertaken in coconut; however, comprehensive data on the structure, molecular evolution, expression profiling and functions of TFs in coconut remain elusive. The recent study of Jin et al. (2021) has revealed the presence of 23 *ARF*s in the oil palm (*Elaeis guineensis* Jacq.) genome. In view of the importance of the ARFs in both the plant growth development and their participation in responses to various stress conditions, this investigation performs the genome-wide analyses of ARF gene family in coconut. A total of 20 ARF genes were categorized by aligning the whole genome data of Chowghat Green Dwarf cultivar with the *ARF* coding sequences of closely related species (date palm and oil palm). Furthermore, phylogenetic relationship, gene structure, domain prediction and expression profiles of 20 *ARF*s in *Cocos nucifera* L. were undertaken. The present work provides a base for understanding the molecular mechanism of ARFs in coconut and establishes a significant foundation for forthcoming investigations aimed at genome-assisted breeding of this perennial species.

2. Materials and methods

2.1. Documentation of ARF genes in coconut

The coding sequences of *ARF*s of plant species sharing close lineage with coconut, viz., oil palm (*Elaeis guineensis*) and date palm (*Phoenix dactylifera*), were downloaded from NCBI database (https://www.ncbi.nlm.nih.gov/) and were used as *ARF* model data set. Using the retrieved *ARF* coding sequences as query, all possible homologous sequences in Chowghat Green Dwarf (CGD) genome (NCBI sequence read archive database: BioProject Number PRJNA413280; Accession Number SRS2696501) were identified by BLAST analysis. The aligned area was further recovered from scaffolds using a custom made Python script (score value of$\geq$100 and e value $\leq 10e{-}^{5}$). Besides, we used the CGD protein sequence in FASTA format as a query to check against Pfam Hidden Markov Model (HMM) library, employing PfamScan tool (https://www.ebi.ac.uk/seqdb/confluence/display/THD/PfamScan). Protein sequences with profiles of ARF protein domains [PF 06507: ARF (AUX_RESP); PF 02309: AUX/IAA family; PF02362: B3 DNA binding domain (B3)] were then extracted. All the putative *Cocos nucifera* ARFs (CnARFs) obtained from BLAST analysis, followed by Pfam searches, were further filtered to eliminate redundant sequences and isoforms. Finally, FGENESH (http://www.softberry.com/) gene prediction tool was also used for the initial annotation of the predicted *CnARF* family, which was further corroborated by employing the NCBI conserved domain database (https://www.ncbi.nlm.nih.gov/Structure/cdd/wrpsb.cgi). For the calculation of molecular weight, theoretical isoelectric point (pI) and polypeptide length, ExPASy ProtParam tools (https://web.expasy.org/protparam/) were used.

2.2. Phylogenetic analysis and amino acids composition of CnARFs

Multiple sequence alignment was performed with predicted ARF proteins sequences obtained from coconut (CnARF), date palm (PdARF) and oil palm (EgARF) in ClustalW2 (https://www.ebi.ac.uk/Tools/msa/clustalw2/). The gap open penalty parameter was set as 15; gap extension penalty parameter as 5 and the weight matrix selected was 'IUB' for DNA. Phylogenetic tree was generated using the multiple-aligned ARF protein sequences in MEGAX (https://www.megasoftware.net/) software following the neighbor-joining (NJ) method (Saitou and Nei, 1987). The test of phylogeny was performed with 1000 bootstrap replications, and the evolutionary distances were calculated following the Poisson correction technique (as given in Die et al., 2018). ARFs with a single lineage at the base constituting a common predecessor were further grouped together to create subclasses. Maximum Likelihood method, with the JTT matrix-based model, was used to create a global phylogenetic tree, using MEGAX, to show the relationship of CnARFs with select plant species, viz., *O. sativa* (txid:4530), *Z. mays* (txid:4577), *P. dactylifera* (txid:42345),*Camellia sinensis* (txid:4442), *Jatropha curcas* (txid:180498),*Cicer arietinum* (txid:3827), *Musa acuminata* (txid:4641) and *E. guineensis* (txid:51953). The bootstrap test was conducted with 1000 repetitions.

To analyze the amino acid distribution pattern in three distinct

domains of coconut ARFs, a multiple sequence alignment was performed employing MEGAX (https://www.megasoftware.net/), and generation of the shaded printouts from the aligned sequences was done using BoxShade (https://embnet.vital-it.ch/software/BOX_form.html). The shaded print outs from BoxShade were used to calculate the theoretical number of activators and repressors. The middle regions of the CnARFs were evaluated for the amino acid composition using specific tools, provided in MEGAX, and histograms were constructed.

2.3. Gene structure and prediction of conserved motifs of CnARFs

The exon-intron architecture of *CnARFs* was obtained from the online Gene Structure Display Server (GSDS) software (http://gsds.cbi.pku.edu.cn/) by comparing the full-length cDNA sequences with its corresponding genomic DNA as described by Hu et al. (2015). The MEME algorithm (http://meme-suite.org/tools/meme) was executed on the grounds of phylogenetic relationship to discover the conserved motifs among the predicted 20 coconut ARF sequences. The program was run locally, and the parameters were set to a maximum of nine motifs and motif width between six and 50 (both inclusive). Finally, the MAST program was utilized to explore all the detected motifs in CnARF proteins.

2.4. Prediction of protein–protein interaction of CnARFs

The STRING database (Search Tool for the Retrieval of Interacting Genes/Proteins; https://string-db.org) was utilized to examine protein-protein interaction (PPI) of predicted CnARFs and other related proteins. Date palm (*P. dactylifera*) was selected as a query organism, and the PPI network was constructed with a confidence score of at least 0.400 and the interaction was displayed in Cytoscape.

2.5. Imposition of abiotic stresses and treatment with growth regulators

Expression analysis of *CnARF*s in mature zygotic embryos, under imposed abiotic stresses, was undertaken as described below. Briefly, zygotic embryos, along with coconut endosperm, in the form of endosperm cylinders, were removed using a cork borer from the split-open matured nuts of CGD palms grown at the Experimental Farm, ICAR-CPCRI, Kasaragod, Kerala, India (12°31′41.1″N, 74°58′06.9″E). The endosperm cylinders, containing the embryos, were washed thrice in distilled H_2O and further surface sterilized with 0.01% $HgCl_2$ for 3 min. The traces of $HgCl_2$ were washed again by rinsing the treated cylinders with sterile distilled H_2O thrice. Embryos were removed from endosperm cylinders using a sterile scalpel, under aseptic conditions, and sterilized with 20% sodium hypochlorite solution for 20 min, followed by rinsing 4–5 times with sterile distilled H_2O. Sterile embryo explants were initially cultured in Y3 basal medium (Eeuwens, 1976) to which 3% (*w/v*) sucrose and 0.1% (*W/V*) activated charcoal were added. The cultures were maintained under complete darkness at 26 °C. The composition of Y3 medium is in provided in Supplementary File 1. After 30 days, 100 embryos with uniform growth and weight were selected and were exposed to temperature, osmotic stresses and growth regulator treatments.

For growth regulator treatments, freshly prepared working solutions of abscisic acid (ABA; 100 μM and 200 μM), salicylic acid (SA; 100 μM and 200 μM), cyclodextrin (CD; 50 μM and 100 μM), indole-3-acetic acid (IAA; 10 μM and 20 μM) and 2, 4-dichlorophenoxy acetic acid (2,4-D; 74.66 μM) were added to the Y3 medium. To impose osmotic stress, embryos were exposed to PEG 6000 [10% (w/v) and 20% (w/v)], NaCl (150 μM and 300 μM) and mannitol (100 μM and 200 μM) treatments, which were supplemented in the Y3 medium. Embryos were also subjected to heat stress (42 °C) and cold stress (4 °C). The test samples were collected at 4, 12, 18, and 24 h after the imposition of hormone treatment; whereas, embryos subjected to osmotic and temperature stresses were sampled at 1, 3, 5, and 7 days after the treatments. The samples were flash-frozen in liquid nitrogen for RNA extraction and gene expression profiling studies.

2.6. Total RNA extraction and cDNA synthesis

Total RNA was extracted from the frozen embryos and inoculated leaflets, sampled at specific time intervals after imposition of treatments, using NucleoSpin® RNA Plant kit (Macherey-Nagel) following the manufacturers' instructions. To check the quantity and quality of isolated RNA, samples were subjected to a 1% agarose gel electrophoresis, and RNA integrity number (RIN) was examined using an Agilent Technologies 2100 Bioanalyzer using the Agilent RNA chip. Reverse transcription of total RNA was accomplished utilizing the Prime Script 1st strand cDNA Synthesis Kit (Takara). The concentration of cDNA was quantified by spectrophotometric measurement (ND-1000 Nano Drop technologies).

2.7. Quantitative reverse transcription PCR (qRT-PCR) and expression analysis

Initially, PCR primer sets were designed for 20 *CnARF*s using Primer3web version 4.1.0 server (http://primer3.ut.ee/). The primers for the selected *CnARF*s were designed with minor modifications to the default parameters of the Primer3web (melting temperature: 51–62 °C, primer length: 19–25 nucleotides, product size: 80–160 bp and GC content: 40–55%). The quality and specificity of the designed primers were determined by gel electrophoresis. From the total of 20 primer sets, only 10 primer pairs, producing single discrete bands were finally selected for expression profiling using qRT-PCR. Supplementary File 2 lists the primer sequences.

The expression patterns of RNA transcripts were quantified utilizing the Step One Real-Time PCR System (Applied Biosystems). The reaction cocktail comprised of 50 ng of diluted cDNA as the template, 5 μl of Power SYBR Green PCR Master Mix (Applied Biosystems) and 2 μl of sequence-specific primers and the final reaction mixture was made up to a total volume of 10 μl by adding nuclease-free water. All the qRT-PCR analysis was performed with two biological replicates and three technical replicates. The PCR program was as follows: 95 °C for 10 min, followed by 40 cycles of 95 °C for 15 s, 55 °C for 1 min. Amplification of coconut elongation factor-1 alpha (EF-1∞) gene was taken as the internal control (Xia et al., 2014; Rachana and Rajesh, 2019). The relative fold change in gene expression was computed using the $2^{-\Delta\Delta CT}$ method (Livak and Schmittgen, 2001). Statistical analysis was performed using SPSS 16.0 software (SPSS Inc., Chicago, IL, USA). Single sample *t*-test ($P < 0.05$) was employed for the calculation of the significant differences in the relative expression of specific *CnARF*s between the control and treated samples. Expressional fold-changes greater than 2 (*P*-value of <0.05) were considered as the up-regulated genes and fold changes of 0.5 or less was used to define genes which were down-regulated genes (*P*-value of <0.05).

3. Results

3.1. Genome-wide identification of coconut ARFs

Initially, a total of 117 candidate *ARF*s (*CnARF*s) were predicted in the dwarf coconut (CGD) genome using a combination of BLAST searches, HMM profiling and domain analysis approach. After filtering out the redundant sequences and isoforms, a total of 20 potential *ARFs* were identified in the CGD genome. The nomenclature of *ARF*s in this study is based on the homology among *EgARF* (*ARF*s from oil palm), *PdARF* (*ARF*s from date palm) and *CnARF* as the confirmed *ARF*s of coconut were derived from the model data set consisting of oil palm and date palm ARFs. The details of these 20 *CnARF*s, including gene name, ORF length, features of introns, location of specific domains, and polypeptide characteristics are enlisted in Table 1. Further, validation of all

Table 1
Information of ARF family genes in coconut.

Sl. no.	Coconut ARF genes	No. of exons	ORF (bp)	Predicted peptide length (aa)	Position of B3 domain	Position of ARF domain	Position of Aux/IAA domain	Iso-electric point	Molecular weight (Da)
1.	*CnARF1*	11	2385	475	173–267	261–325	404–435	5.00	53,170.74
2.	*CnARF2*	13	2319	773	123–224	249–331	664–773	6.40	86,780.48
3.	*CnARF3*	12	2295	764	123–190	215–297	628–722	6.70	85,086.07
4.	*CnARF4*	12	2394	650	170–271	295–375	505–527	6.17	71,362.21
5.	*CnARF5*	12	1713	570	128–223	216–281	497–537	5.72	63,495.29
6.	*CnARF6*	11	1590	600	41–141	167–249	459–562	6.16	66,881.39
7.	*CnARF7*	12	1848	615	83–183	209–263	444–597	6.13	68,552.81
8.	*CnARF8*	6	663	353	45–105	154–233	275–319	6.63	39,702.35
9.	*CnARF9*	12	2190	729	53–154	179–262	623–718	5.87	81,871.20
10.	*CnARF10*	12	2190	729	53–154	179–262	623–718	5.87	81,871.20
11.	*CnARF11*	9	1779	593	44–145	171–251	–	8.41	65,868.90
12.	*CnARF12*	13	2001	666	58–159	184–265	–	8.74	74,148.09
13.	*CnARF13*	2	954	802	–	9–91	707–785	5.83	89,756.47
14.	*CnARF14*	12	2283	829	112–213	238–321	–	6.41	92,440.84
15.	*CnARF15*	15	2685	894	123–224	249–332	755–847	6.31	98,873.10
16.	*CnARF16*	2	2055	684	125–226	295–378	619–656	6.61	74,463.47
17.	*CnARF17*	8	1302	615	83–183	209–263	444–597	6.13	68,552.81
18.	*CnARF18*	15	2742	1153	128–247	272–355	1013–1083	8.14	128,492.82
19.	*CnARF19*	15	2844	1125	128–229	254–337	990–1077	6.75	125,280.41
20.	*CnARF20*	11	2169	722	81–148	173–255	586–680	7.11	80,402.79

the predicted ARF protein sequence was undertaken using the Conserved Domain Database and Pfam protein motif analyses. The length of the deduced CnARF proteins markedly varied from 353 amino acids (CnARF8) to 1153 amino acids (CnARF18). The corresponding molecular weight varied from 39,702.35 Da (CnARF8) to 128,492.82 Da (CnARF18) with the predicted isoelectric point in the range of 5.00 (CnARF1) to 8.74 (CnARF12) suggesting differential sub-cellular domain function (Table 1).

3.2. Molecular phylogeny, conserved domains and protein structure of CnARFs

The evolutionary analysis of CnARFs, along with EgARFs and PdARFs, and phylogeny reconstruction revealed that all the ARF genes clustered into three major classes viz., I, II and III, with each class, in turn, subdivided into two subgroups, 'A' and 'B' (Fig. 1). Class I comprised of 16 members (including seven from coconut), Class II had 10 members (including four from coconut), and Class III comprised a total of 19 members (including nine from coconut). Moreover, a total of 13 sister pairs were documented in the phylogenic plot, with proteins that clustered together with high bootstrap value (>65%) being

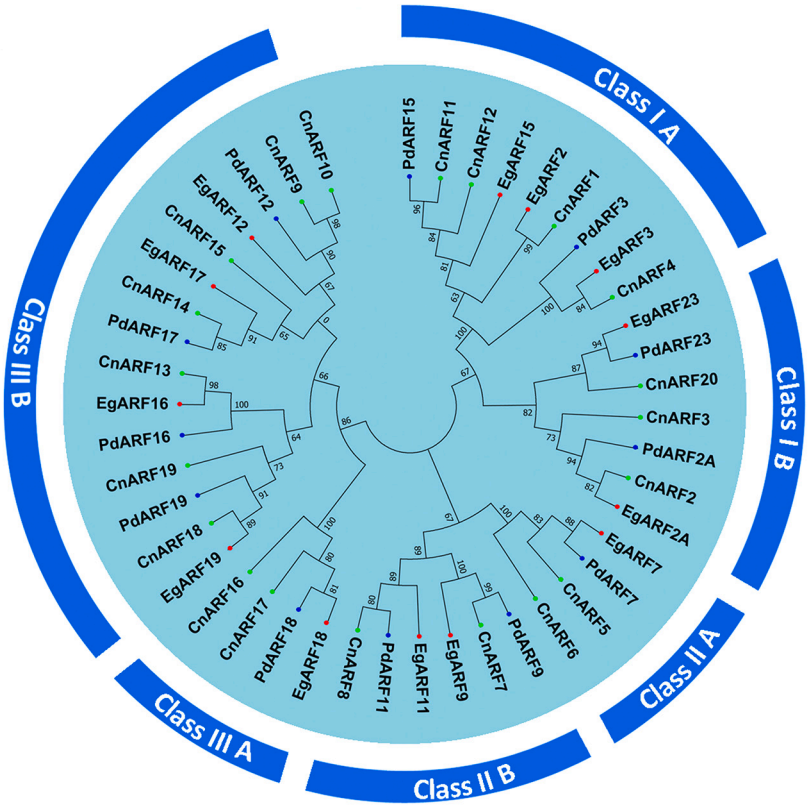

Fig. 1. Phylogenetic studies of ARFs from coconut, oil palm and date palm, carried out employing the Neighbor-Joining (NJ) method. The phylogenetic tree was generated by using MEGAX software and the reliability of the phylogenetic tree was accessed using 1000 bootstrap replicates. The bootstrap values are specified for all branches. Forty-five genes were classified into six sub-groups viz., Ia, Ib, IIa, IIb, IIIa and IIIb. Green color solid round indicates 20 coconut ARF proteins (CnARF), red color solid round indicates 13 oil palm ARF proteins (EgARF) and blue color solid round indicates 12 ARF proteins from date palm (PdARF). (For interpretation of the references to color in this figure legend, the reader is referred to the web version of this article.)

considered as sister pairs (four pairs of PdARF-CnARF, five pairs of EgARF-CnARF, three pairs of EgARF-PdARF and a pair of CnARF-CnARF). The global phylogenetic tree, created utilizing the Maximum Likelihood method, to show the relationship of CnARFs with select plant species, is provided as Supplementary File 3.

Analyses of exon/intron distribution and conserved motifs are imperative to explore the structural evolution and functional diversity among the *CnARFs* of coconut. Coding sequences of *CnARF*s are interrupted by the introns. The exon number varied from 2 to 15 (Fig. 2). The exon/intron distribution pattern was found to be quite similar among some of the sister pair in the phylogenetic tree. The conserved motifs in coconut ARFs, analyzed using MEME algorithm, divulged nine conserved motifs in coconut ARFs (Fig. 3) and all of them could be annotated using the Pfam. Motifs 1 and 2 were identified as B3 DNA binding domain, which specifically recognizes and binds the auxin-responsive element (AuxRE) at the promoter region of the auxin-responsive genes. Motifs 6, 9 and 3 correlated with the ARF domain. The ARF domain can vary according to the amino acid composition of the middle region, and it largely determines the uniqueness of ARFs. The CTD domain (domain III/IV) was identified by motifs 5 and 7. Overall, the MEME analysis revealed that 16 (of Classes I, II and III) among the 20 CnARFs possessed all the three principal domains (amino-terminal DNA binding domain with plant-specific B3 type sub-domain, an ARF sub-domain and an AUX /IAA sub-domain) characteristic of all the ARF proteins. Interestingly, three CnARFs genes possessed only B3 and ARF domains, suggesting that 15% of CnARFs lacked CTD. Since the middle region (MR) of ARFs showed maximum variation compared to the other two domains, the amino acid configuration of the middle region was analyzed using MEGAX and BoxShade (Supplementary File 4). Presence of glutamine (Q) enriched zone was observed among the five CnARFs (CnARF2, CnARF3, CnARF7, CnARF17 and CnARF20). Functional diversity of the remaining CnARFs can be interpreted based on the characteristics of the CTD domain and MR domain. A total of 12 ARFs with CTD and three without CTD possessed an abundance of amino acids residues such as serine (S), proline (P), glycine (G) and leucine (L) in their MR region (Supplementary File 5).

3.3. Interaction network of CnARF family

The CTD domain of ARFs exhibits a strong propensity for dimer formation with other cellular proteins (specifically AUX /IAA) and also between the ARFs. The interaction network analysis involving ARFs and other cellular components using the online STRING algorithm disclosed nine interactive proteins with a high confidence score greater than >0.04. The functional partners of ARF family network in coconut are IAA10, IAA16, IAA1, IAA30, MYB44, Aux22D, KAN4, BHLH79 and AP2 (Table 2, Fig. 4). Moreover, IAA30, IAA1 and CnARF18 were found to be connected with several other ARFs and transcription factors, placing IAA at the core of the interaction network. The interaction network of CnARF18, CnARF14 and CnARF15 were not only limited to IAA, but it extended to other ARFs.

3.4. Expression profiling of CnARFs in zygotic embryos after imposition of osmotic stress

Expression of *CnARF*s was studied in coconut zygotic embryos subjected to osmotic stresses for 1, 3, 5 and 7 days post-treatment. *CnARF4* was significantly induced under osmotic stresses. Expression of six *CnARF*s (viz., *CnARF5*, *CnARF8*, *CnARF9*, *CnARF13*, *CnARF14* and *CnARF18*) were markedly down-regulated at all the time periods tested following PEG 6000, NaCl and mannitol treatments. Though, the responses were not linear with time intervals, *CnARF6, CnARF12, CnARF4 and CnARF10* were up-regulated at some point of treatment whereas *CnARF6* and *CnARF12* showed mixed responses. All the other *CnARF*s were suppressed, indicating that the response of *CnARF*s to osmotic stresses might be complex (Fig. 5).

3.5. Expression of CnARFs under induction of temperature stress

All *CnARF*s, except *CnARF8* and *CnARF12,* showed up-regulation following heat or cold treatments. However, the responses were not sequential with the exposure time periods in both treatments. Interestingly, all *CnARFs* responded similarly at 24 h after treatment (HAT) with significant down-regulation. *CnARF9* up-regulated to the tune of 4 and

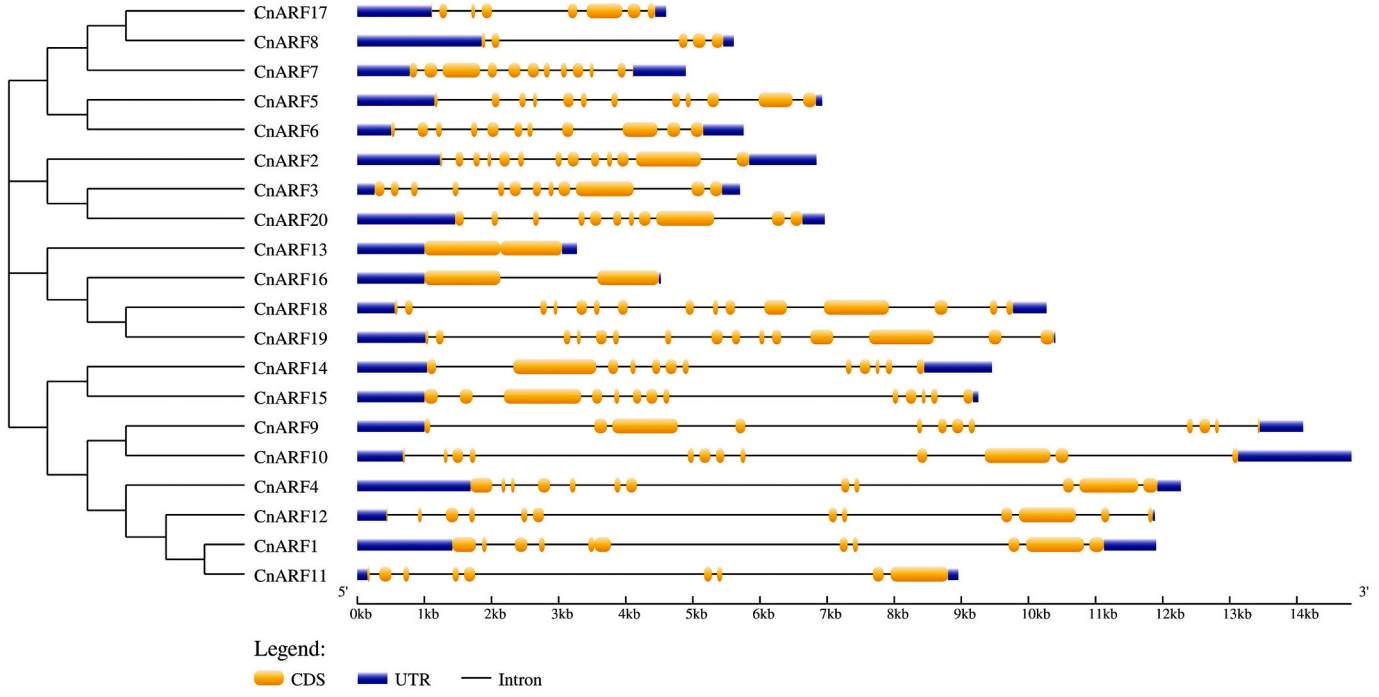

Fig. 2. Phylogenetic relationships and exon-intron architecture of *CnARF*s. (A) Phylogenetic relationship among *CnARF*s (B) exon-intron architecture of CnARFs. The exons and introns are depicted as boxes and lines, respectively.

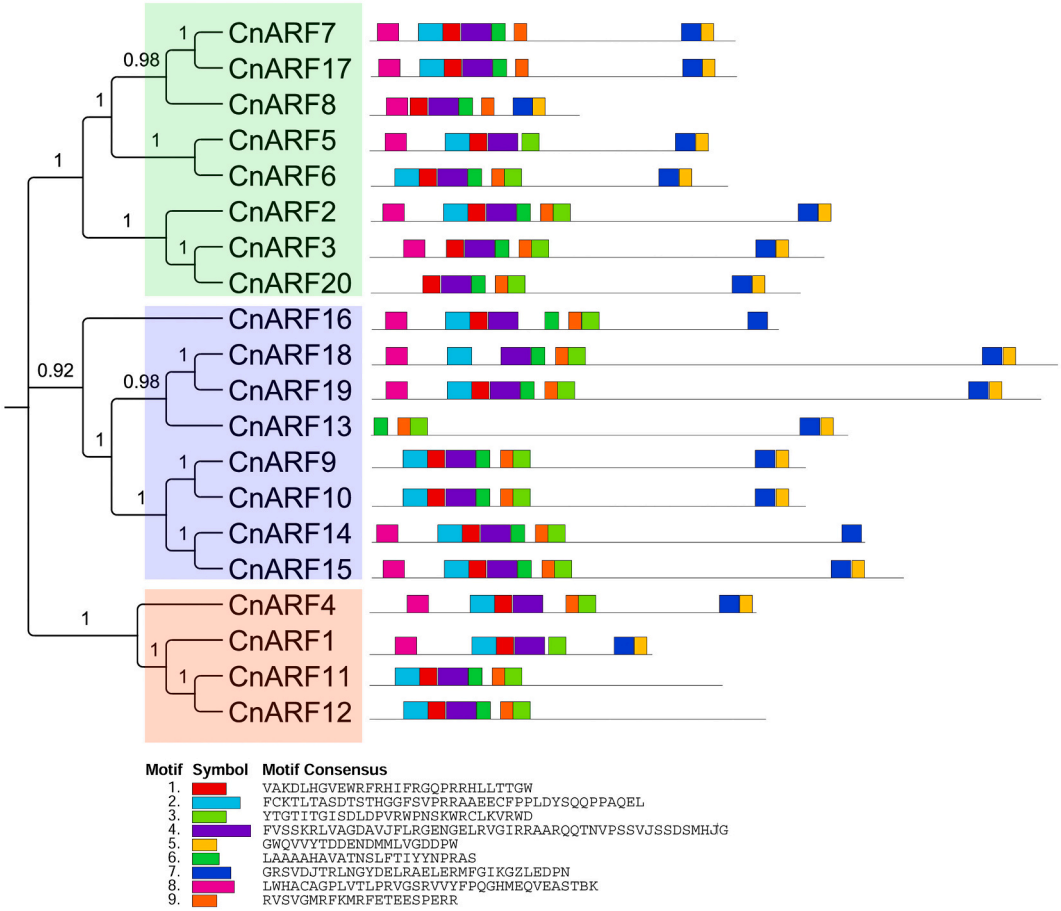

Fig. 3. Phylogenetic relationships and conserved motifs of CnARFs. (A) Phylogenetic relationship among CnARFs (B) Conserved motif analysis of CnARFs. Different motifs are depicted by specific color, and the particulars of the conserved motifs are shown.

Table 2
Proteins in *P. dactylifera, A. thaliana, Z. mays* and *O. sativa* which appear to match the query CnARFs. The STRING parameters of closest proteins, identity percentages and bit scores are provided.

Sl. no.	Coconut ARFs	*Phoenix dactylifera*			*Arabidopsis thaliana*			*Zea mays*			*Oryza sativa*		
		STRING protein	Identity	Bit score	STRING protein	Identity	Bit score	STRING protein	Identity	Bit score	STRING protein	Identity	Bit score
1.	**CnARF1**	XP_008808072.1	51.3	642.9	ETT	53.7	414.5	103,630,727	55.1	448.7	ARF15	55.2	453
2.	**CnARF2**	XP_008776920.1	88.6	1390.2	ARF2	56.9	803.1	100,274,571	59.5	828.2	ARF4	60.6	853.2
3.	**CnARF3**	XP_008811924.1	78.9	1303.1	ARF2	52.1	730.3	100,274,564	52.2	722.2	ARF24	50.4	731.5
4.	**CnARF4**	XP_008783126.1	73	1034.2	ETT	63.7	520.8	103,630,727	57.5	563.5	ARF15	57.7	575.1
5.	**CnARF5**	XP_008795276.1	81.2	959.1	At1g59750	54	628.6	arftf36	62.3	672.9	ARF7	61.7	701.8
6.	**CnARF6**	XP_008786460.1	88.7	1009.6	At1g59750	65.5	709.5	arftf36	69.4	740	ARF7	70.2	795.4
7.	**CnARF7**	XP_008808096.1	76.5	978	ARF9	51	579.3	103,646,418	50.5	529.3	ARF1	49.2	563.9
8.	**CnARF8**	XP_008807235.1	40.4	406.8	ARF18	37.3	325.1	103,646,418	31.3	255.4	ARF7	31.4	255.8
9.	**CnARF9**	XP_008813049.1	90.3	1308.9	ARF8	59.1	805.8	arftf3	69.4	991.5	ARF12	70.2	979.9
10.	**CnARF10**	XP_008813049.1	90.3	1308.9	ARF8	59.1	805.8	arftf3	69.4	991.5	ARF12	70.2	979.9
11.	**CnARF11**	XP_008808072.1	91.3	1100.5	ETT	66.1	434.5	103,630,727	53.4	581.6	ARF15	54.5	586.3
12.	**CnARF12**	XP_008798266.1	88.4	1073.2	ETT	65.9	453.8	103,630,727	53.3	599	ARF15	55.3	617.8
13.	**CnARF13**	XP_008792838.1	83.1	1012.3	ARF19	51.8	495.4	ARF27	62.7	680.6	OsJ_005181	44.5	380.9
14.	**CnARF14**	XP_008794474.1	93.3	1452.2	ARF6	68.7	988.4	ARF16	67.3	1000	ARF6	68.4	1043.1
15.	**CnARF15**	XP_008777704.1	89.1	1574.7	ARF6	65.6	1099	ARF16	67.4	1140.6	ARF17	70.8	1201
16.	**CnARF16**	XP_008785274.1	95	1339.7	ARF16	57.8	717.6	ARF2	63.7	840.9	ARF18	66.8	883.2
17.	**CnARF17**	XP_008808096.1	76.5	978	ARF9	51	579.3	103,646,418	50.5	529.3	ARF1	49.2	563.9
18.	**CnARF18**	XP_008798163.1	91.5	1635.9	ARF19	49.9	755	arftf20	67.1	1113.6	OsJ_005181	64.6	1120.5
19.	**CnARF19**	XP_008801434.1	89.7	1733	ARF19	51	833.6	arftf20	67.1	1192.2	OsJ_005181	66.7	1221.1
20.	**CnARF20**	XP_008811924.1	74.4	1196.4	ARF2	51.4	654.8	100,274,564	50.9	655.6	ARF24	48.9	666.8

3.5 folds in heat and cold treatments, respectively. Also, expression of *CnARF4* and *CnARF6* were enhanced after 4–12 HAT when subjected to high-temperature treatment, whereas *CnARF13* and *CnARF10* were up-regulated only at 12 HAT (Fig. 6).

3.6. Expression profiling of CnARFs in zygotic embryos following growth regulator treatment

Molecular responses of 10 *CnARFs* to external auxin stimuli,

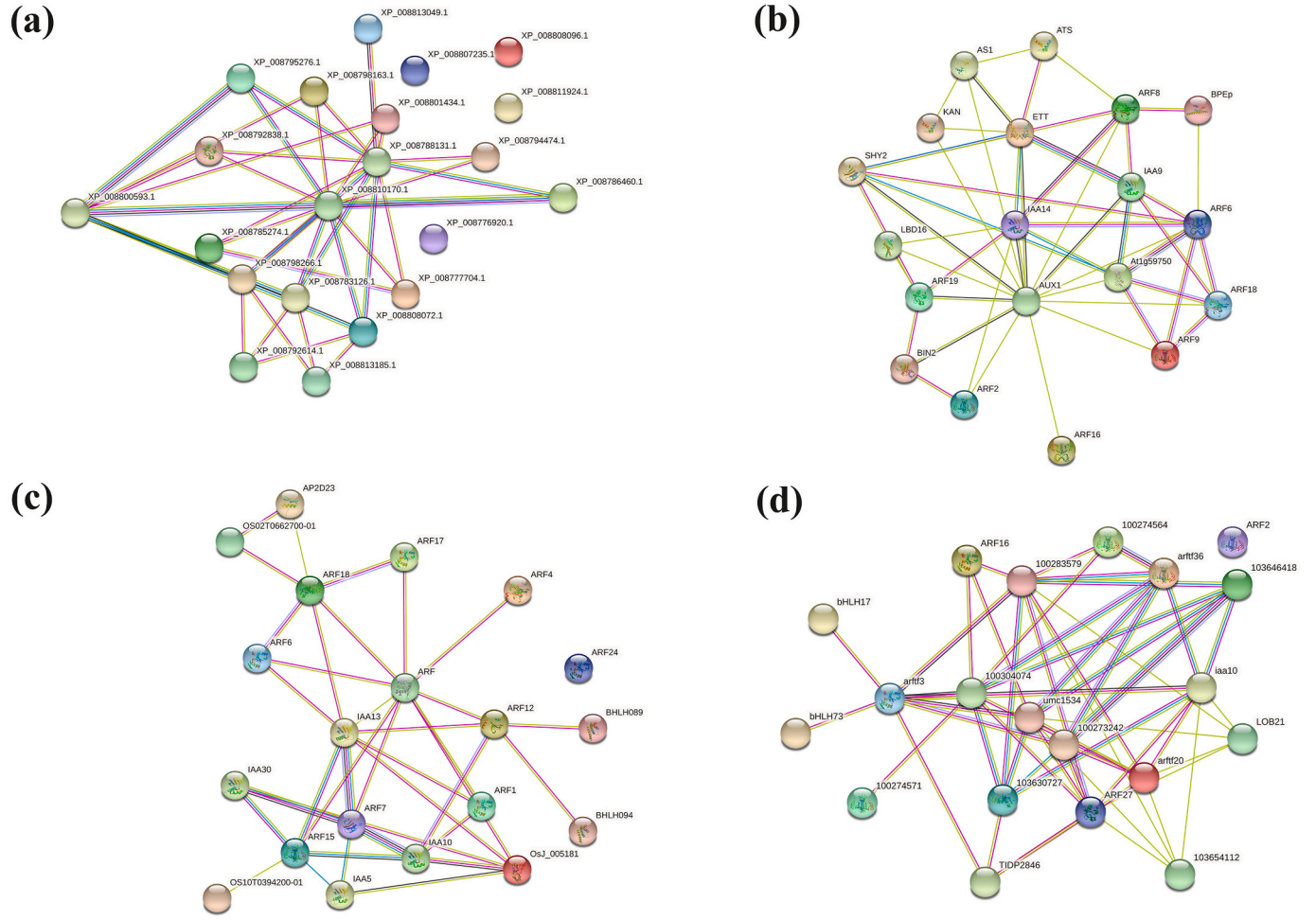

Fig. 4. Association network among closest BLAST hits of *Phoenix dactylifera*, *Arabidopsis thaliana*, *Oryza sativa* and *Zea mays* resulting from CnARF proteins used as query in multiple sequences in STRING.
(a) *P. dactylifera*: Nodes (nos.) = 21, Edges (nos.) = 38, Node degree (average) = 3.62, Local clustering coefficient (average) = 0.113, Number of edges (expected) = 5, and PPI enrichment *P*-value of $<1.0e^{-16}$. (b) *A. thaliana*: Nodes (nos.) = 19, Edges (nos.) = 50, Node degree (average) = 5.26, Local clustering coefficient (average) = 0.571, Number of edges (expected) = 11, and PPI enrichment *P*-value of $<1.0e^{-16}$. (c) *O. sativa*: Nodes (nos.) = 20, Edges (nos.) = 36, Node degree (average) = 3.6, Local clustering coefficient (average) = 0.476, Number of edges (expected) = 10, and PPI enrichment *P*-value of $<3.52e^{-10}$. (d) *Z. mays*: Nodes (nos.) = 20, Edges (nos.) = 53, Node degree (average) = 5.3, Local clustering coefficient (average) = 0.291, Number of edges (expected) = 10, and PPI enrichment *P*-value of $<1.0e^{-16}$.

following treatment of zygotic embryos with IAA and 2,4-D, revealed that two *CnARFs* (viz., *CnARF6* and *CnARF12*) were up-regulated within 4 h after treatment (HAT) with 10 μM/ 20 μM of IAA and the peak expression was maintained till 18 HAT, after which the expression ceased. Eight *CnARFs* (viz., *CnARF5*, *CnARF8*, *CnARF9*, *CnARF13*, *CnARF14*, *CnARF18*, *CnARF4* and *CnARF10*) were found to be suppressed across all the time points following IAA treatment. On the other hand, two genes, *CnARF10* and *CnARF13,* were significantly induced by 2, 4-D and the expression level of *CnARF10* declined at 24 HAT. Among the down-regulated genes, *CnARF8* and *CnARF14* were constantly suppressed during 4, 12, 18 and 24 HAT whereas *CnARF13* which did not undergo any remarkable change until 18 HAT was distinctly induced at 24 HAT (Fig. 7).

Surprisingly, none of the 10 *CnARFs* was induced following the application of ABA. Among the suppressed ARFs genes, six (viz., *CnARF5*, *CnARF8*, *CnARF9*, *CnARF13*, *CnARF14* and *CnARF18*) were found to be significantly down-regulated at all the time points. Also, a few *CnARFs* showed a similar kind of expression pattern after treatment with SA and CD. ARFs such as *CnARF5* and *CnARF6* showed induced expression only at 12 HAT, whereas *CnARF12* and *CnARF10* showed little change in expression till 18 HAT and were fully suppressed at 24 HAT with ABA. Conspicuously, five genes (viz., *CnARF8*, *CnARF9*, *CnARF13*, *CnARF14* and *CnARF18*) were down-regulated during the time period studied under SA and CD treatment (Fig. 7).

4. Discussion

Coconut (*Cocos nucifera* L.) is an important perennial crop grown in the tropical and sub-tropical regions of the world. Almost every part of the coconut tree is utilized by rural communities (Arunachalam and Rajesh, 2008, 2017). The phytohormone auxin governs various developmental processes and plants' response to the adverse environmental conditions by altering a set of auxin-responsive genes. These auxin-dependent cellular signaling pathways are mediated through a class of TFs called ARFs (Guilfoyle and Hagen, 2007; Di et al., 2016; Guilfoyle, 2015). Genome-wide characterization and expression profiling of ARFs in model species such as *Arabidopsis* (Okushima et al., 2005), *Medicago truncatula* (Shen et al., 2015), annual crops of economic importance such as *Oryza sativa* (Wang et al., 2007), *Zea mays* (Xing et al., 2011), *Lycopersicum esculentum* (Zouine et al., 2014), *Cicer arietinum* (Die et al., 2018) and perennials namely *Citrus sinensis* (Li et al., 2015), *Musa acuminate* (Hu et al., 2015), *Jatropha curcas* (Tang et al., 2018), *Prunus*

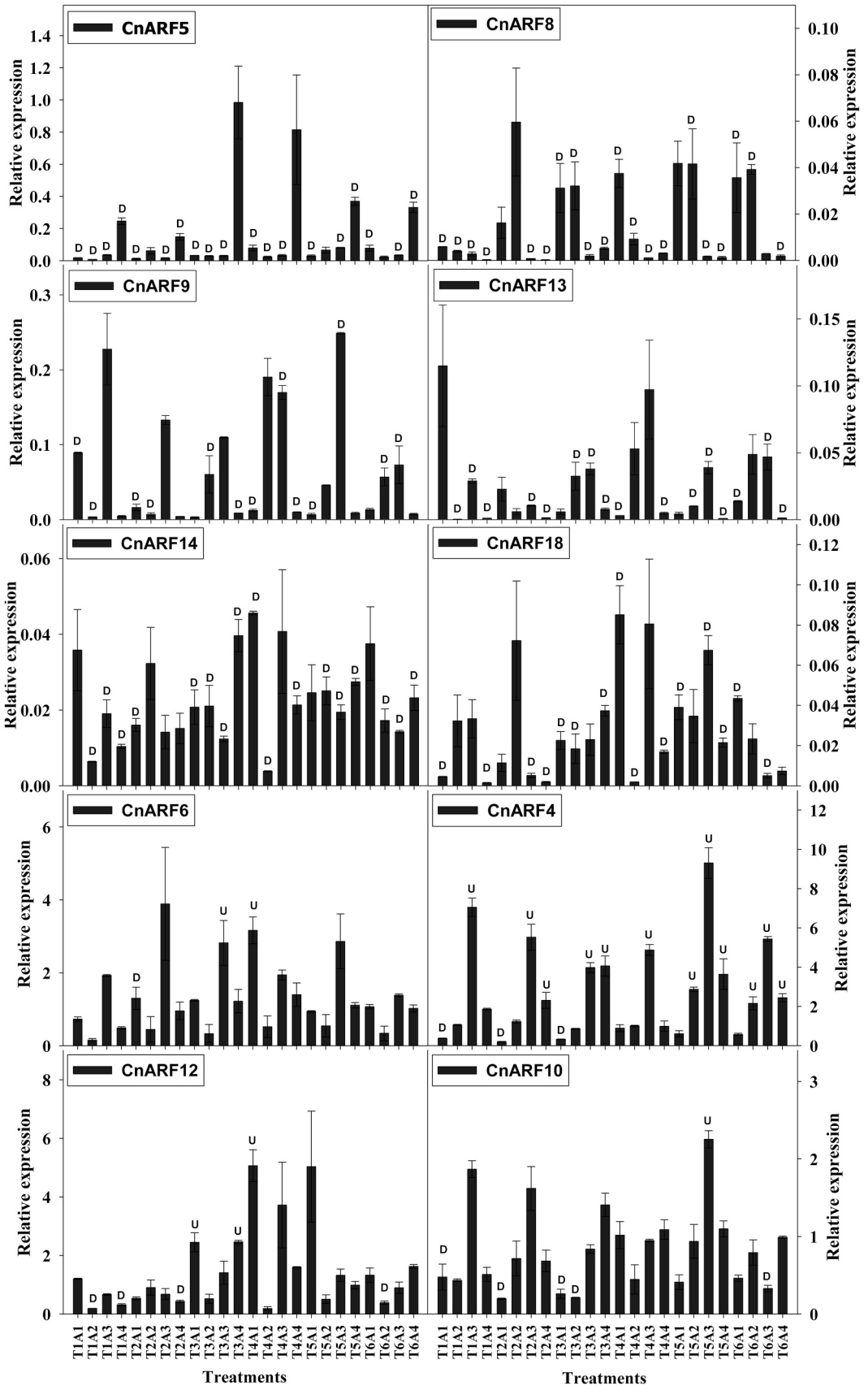

Fig. 5. Expression profiles of 10 *CnARF*s in coconut zygotic embryos after imposition of osmotic stresses. T1 to T6 corresponds to different treatments (T1: PEG 6000–10% (*w/v*); T2: PEG 6000-20% (w/v); T3: NaCl-150 μM; T4: NaCl-300 μM; T5: mannitol-100 μM; T6: mannitol-200 μM). Number of days intervals were represented by A1-A4 (A1: 1st day; A2: 3rd day; A3: 5th day; A4: 7th day after treatment). Each value is a mean of six replications and represented with standard error of mean. Vertical bars denoted with "D" and "U" represents down-regulation and up-regulation during treatment exposure according to single sample *t*-test.

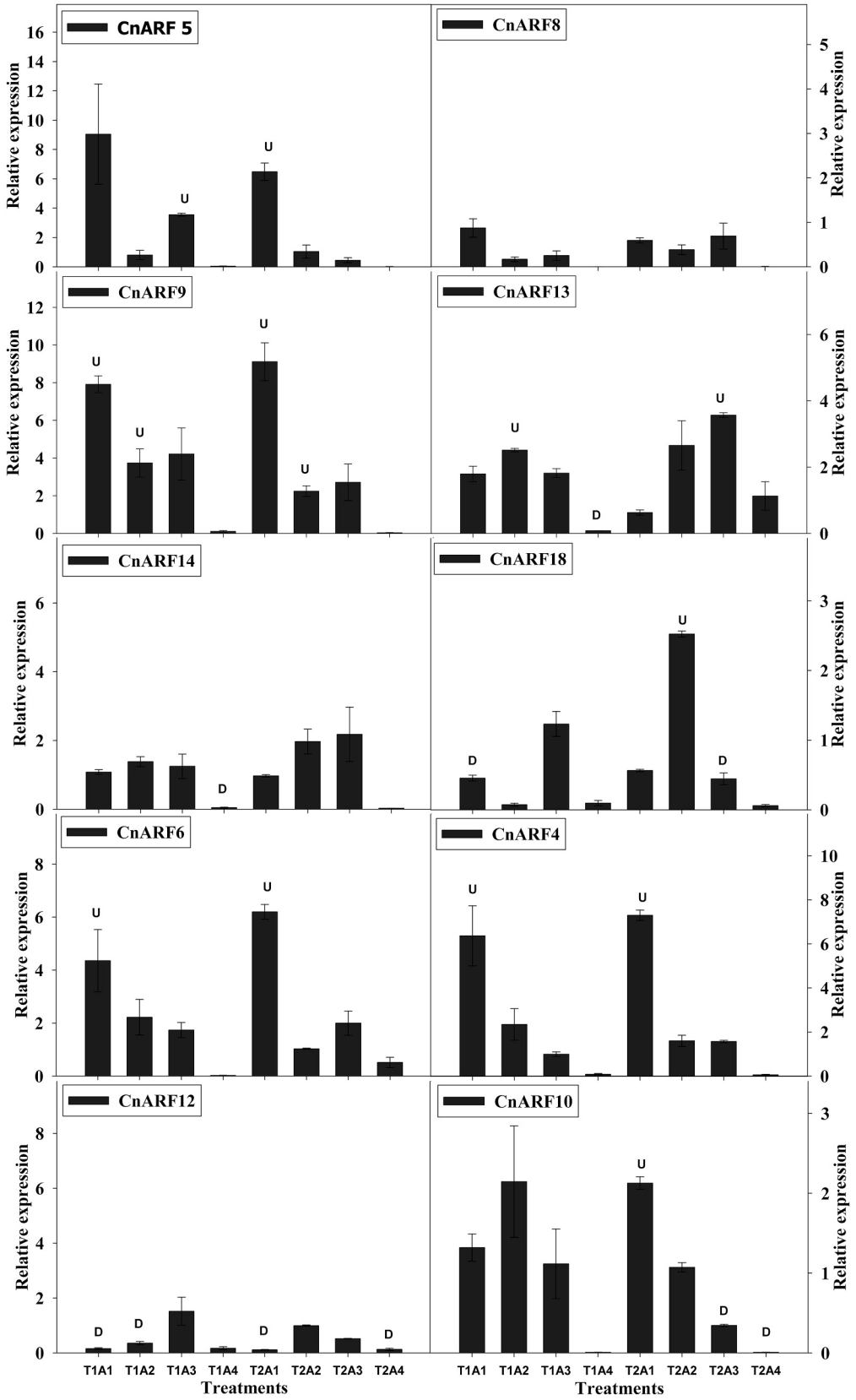

Fig. 6. Expression profiles of 10 *CnARF*s in coconut zygotic embryos under two temperature regimes. T1 represent high temperature- 42 °C, while T2 corresponds to low temperature- 4 °C. The treatment exposure time intervals are represented by A1 - A4 (A1–4 h; A2–12 h; A3: 18 h; A4–24 h). Each value is a mean of six replications and represented with standard error of mean. Vertical bars denoted with "D" and "U" represents down-regulation and up-regulation during treatment exposure according to single sample t-test.

sibirica (Niu et al., 2018) and *Litchi chinensis* (Zhang et al., 2019), underlines the molecular significance of this important class of TFs in the plant kingdom. Though coconut is adapted to grow in wide environmental conditions (Ramesh et al., 2020), the molecular adaptive responses of this palm towards external stresses largely remain unexplored until now. In particular, investigations about the coconut TFs are in nascent stage partly ascribed to its relatively deprived/inadequate genomic resources. In this backdrop, we explored the role of *CnARFs* in response to various abiotic stresses and to delineate its major structural characteristic features and evolutionary relationships with related palm species.

We used the genomic resource of in-house generated whole-genome sequence of a dwarf coconut cultivar Chowghat Green Dwarf (CGD) (Rajesh et al., 2020) to investigate the ARFs of this economically important palm. A total of 20 ARF gene family members were detected from the CGD genome which is comparable to that of *Citrus sinensis* (19) (Li et al., 2015) and *Brachypodium distachyon* (19) (Liu et al., 2018a), *Arabidopsis* (23) (Okushima et al., 2005), and *O. sativa* (25) (Wang et al., 2007). In contrast, the expanded gene members of ARFs documented in *Musa acuminate* (47) (Hu et al., 2015), *Brassica napus* (67) (Wen et al., 2019) and *Triticum aestivum* (52) (Gidhi et al., 2020); could imply that coconut genome has not undergone an extensive duplication and diversification event during its early evolution stage.

Analysis of molecular evolutionary relationships among the ARFs of related palm species divulged the close proximity of CnARFs with that of date palm and oil palm. Furthermore, the discovery of a large number of sister pairs of ARFs among the three palms reinforces the phylogenetic proximities of coconut with oil palm and date palm, which corroborates the traditional view of evolutionary lineage of palms (Barrett et al., 2019). Additionally, phylogeny construction utilizing the full-length protein sequences of CnARFs illustrated three distinct classes (Class I through Class III) characteristics of palm families. Unlike the ARFs characterized in *Arabidopsis* (Okushima et al., 2005), *O. sativa* (Wang et al., 2007), *G.* max (Van Ha et al., 2013), *L. esculentum* (Zouine et al., 2014), *T. aestivum* (Gidhi et al., 2020) and *E. guineensis* (Jin et al., 2021), which showed four distinct clades in their phylogenetic classification, ARFs of coconut could be categorized into three classes. The irregularity in the pattern of branch distribution observed in Class I, II and III of the evolutionary tree suggests molecular diversity. The unusual branch length displayed by CnARF16 of Class II could be attributed to the prolonged period of gene differentiation.

Structural genomic analysis of *CnARFs* revealed a great number of exons (2–15) compared to that of *C. sinensis* (2–14) (Li et al., 2015), *J. curcas* (3–14) (Tang et al., 2018), *L. chinensis* (2–16) (Zhang et al., 2019) and *E. guineensis* (2−13) (Jin et al., 2021). Nonetheless, scrutiny of *M. acuminate* ARFs showed a remarkable number of exons (5–21) exemplifying the wide structural variation and suggesting the significant genome change during its evolution (Hu et al., 2015). The conserved exon-intron structure shared between the sister-pairs of ARFs further lends credence to the phylogenetic relationship among the palms. Similarly, conserved exon-intron structures among the same families of ARFs not only supported their evolutionary relationship but also corroborated their molecular classification (Tang et al., 2018; Wen et al., 2019).

Furthermore, analysis of the conserved motifs indicated that CnARFs belonging to the same class might possess similar regions. Functional domain analysis of CnARF proteins was performed in light of the fact that a typical ARF protein comprises a conserved N-terminus DBD, a variable MR, and C-terminus dimerization domain (CTD) (reviewed in Weijers and Wagner, 2016). Even though all the CnARFs described in this report have a distinct DBD suggesting their prominence in the cellular signal transduction processes, a considerable fraction of CnARFs (15%) were characterized with the truncated CTD. This proportion of truncated CTD among CnARFs is relatively less than those in *Arabidopsis* (17.39%), *B. rappa* (22.58%), *B. distachyon* (23%), *O. sativa* (24%), *L. esculentum* (28.57%), M. *acuminate* (28%) and *L. chinensis* (41%) (Li et al., 2015; Zhang et al., 2019). Nevertheless, the relative preponderance of truncated CTD among the CnARFs suggests their functional incompetence to respond to auxin and numerous auxin-responsive genes. It is also pertinent to recognize that truncated CTD could functionally influence the interaction of other TFs with ARF (Li et al., 2016). Evidence also revealed that the composition of amino acids of MR domain is decisive for its action as an activator or a repressor (Tiwari et al., 2003). Five members of CnARFs have glutamine-rich (D) MRs implying their potential role as the activators of transcription since an abundance of glutamine is a hallmark of ARF activators in all plant lineages. In contrast, a greater proportion of CnARFs (15) showed the abundance of amino acids residues such as serine (S), proline (P), glycine (G) and leucine (L) in their MR region suggesting their principal role as transcriptional repressors. Similarly, structural domain analysis of ARFs has documented the dominance of repressor ARFs over the activators in tea (Xu et al., 2016), allopolyploid species *B. napus* (Wen et al., 2019), and *J. curcas* (Tang et al., 2018). The output from the network analysis shows numerous protein-protein interactions between CnARF and AUX/IAA, which accentuates the prominent role of ARF in the auxin signaling pathway (Fig. 6).

Transcript expression profiling can aid in screening for candidate *CnARFs* possessing potentially distinct functions. A remarkable down-regulation of *CnARFs* was observed following induction of various osmotic stresses (PEG 6000, NaCl and mannitol) (Fig. 7). However, *CnARF4* was found to be significantly up-regulated during osmotic stress implying the complex and intriguing interplay of ARFs and other stress components in coconut. Investigations delineating the molecular mechanisms underlying phytohormone auxin and osmotic stress cross-talk in the leaves of Arabidopsis suggest that moderate concentration levels of auxin induce leaf growth, whereas, at higher concentrations, the inhibitory effect was documented. Furthermore, the genetic regulation of auxin-induced proliferation of leaves during osmotic stress suggests the prominence of auxin-dependent transcriptional regulation (Kalve et al., 2020). In contrast, the majority of the *CnARFs* were up-regulated following the cold or heat treatments. Similar observations were made in previous studies in rice by Du et al. (2012, 2013); it was reported a substantial increase in endogenous auxin levels in response to heat and cold stresses, but decrease in response to drought stress.

Transcript abundance studies of *CnARFs* in response to exogenous auxin stimuli revealed that *CnARF6* and *CnARF12* were significantly up-regulated within 4 h after treatment (HAT) and the expression continued till 18 h after treatment when embryos were treated with IAA. Even though two ARF gene members viz., *CnARF10* and *CnARF13* are simultaneously induced by the synthetic auxin, 2, 4-D, the differences in their expression profile suggests the functional diversity of *CnARFs*. On the contrary, most of *ARFs* in *B. distachyon* (*BdARFs*) were up-regulated following auxin treatment-irrespective of their nature and also exhibited a homologous expression pattern when physiologically similar phytohormones were administered (Liu et al., 2018a). A similar induction of ARFs following auxin treatment was reported in *M. truncatula* (Shen et al., 2015) and *Z. mays* (Xing et al., 2011). Nevertheless, the expression pattern appears to be consistent with the reports depicting that most ARFs are suppressed in the presence of auxin in woody plants (Yu et al., 2014; Li et al., 2015; Xu et al., 2016). The most apparent reason for this observation could be the difference in the regulatory mechanism of these genes in herbaceous and woody plants. Furthermore, only two members of *CnARF* family viz., *CnARF5* and *CnARF6* were stimulated in response to SA and CD treatment, and none of the 10 *CnARFs* genes was induced following the application of ABA. Liu et al. (2018a) had reported induction of ARFs in leaves of *B. distachyon* following exogenous application of ABA. ABA has been reported to participate in the regulation of tolerance of plants to various abiotic stressors (Raghavendra et al., 2010). Plants perceive the modulations in the external conditions and respond to those stimuli by activating phytohormone-mediated pathways (Park, 2007). For instance, accumulation of auxin due to an external stressor results in the induction of hormones such as ABA and

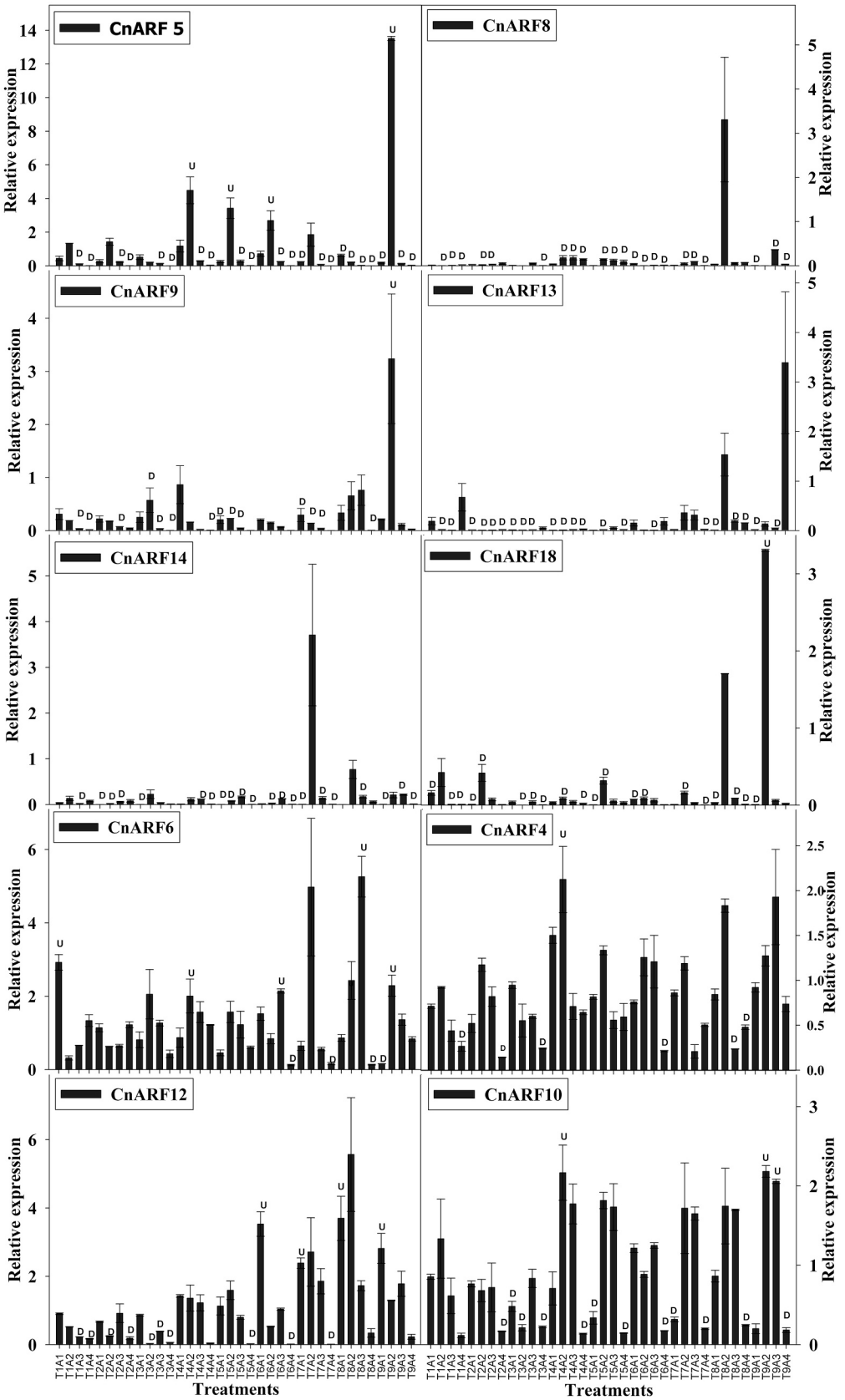

Fig. 7. Temporal variations in expression profiles of 10 *CnARFs* in coconut zygotic embryos in response to growth regulator treatments. T1 to T9 corresponds to different treatments (T1: ABA-100 μM; T2: ABA-200 μM; T3: SA-100 μM; T4: SA-200 μM; T5: CD-50 μM; T6: CD-100 μM; T7: IAA-10 μM; T8: IAA-20 μM; T9: 2, 4-D-74.66 μM). The treatment exposure time intervals are represented by A1 - A4 (A1: 4 h; A2: 12 h; A3: 18 h; A4: 24 h). Each value is a mean of six replications and represented with standard error of mean. Vertical bars denoted with "D" and "U" represents down-regulation and up-regulation during treatment exposure according to single sample t-test.

other metabolic pathways leading to the upregulation of defense-related genes namely C-repeat/dehydration-responsive element-binding factors (CBFs) or responsive to dehydration (RDs) among others (Rock and Sun, 2005; Park et al., 2007). ABA amends the activity of auxin signaling pathway in embryos, thereby reinforces the effect of auxin in repressing the elongation of the embryonic axis. It is accomplished by down-regulating the AUXIN INDUCIBLE (Aux/IAA) gene *AXR2/IAA7* which plays a pivotal role in ABA- and auxin-dependent morphogenesis in the post-germinative growth and development of plants (Belin et al., 2009). Application of auxin regulates the numerous metabolic pathways which are involved in seed secondary dormancy and seed germination. Of particular interest is that auxin-mediated seed dormancy is implicated in epigenetic regulation, thereby enhancing methylation of genomic regions (Matilla, 2020). Thus, this investigation provides a relatively less explored dimension of auxin-mediated transcriptional regulatory control in the seed dormancy and germination processes. In support of our observation, a complex molecular cross-talk between the phytohormones and external stresses such as drought and osmotic stress was proposed based on the expression profile of tea *ARF*s (Xu et al., 2016).

Molecular insights from many studies delineating somatic embryogenesis in *E. guineensis* (Ooi et al., 2012), the fruit abscission in L. *chinensis* (Zhang et al., 2019), fruit setting in L. *esculentum* (Zouine et al., 2014), mesocarp and kernel development in *P. sibirica* (Niu et al., 2018) and fruit development in conjunction with NAA treatment in *Fagopyrum tataricum* (Liu et al., 2018b), have further highlighted the functional versatility of ARF proteins in plant growth and developmental pathways. The observations made in this study convincingly suggest that ARFs, via their modulation of the spatio-temporal expression pattern of stress-responsive genes, could act as potential players capable of mitigating the adverse effects of various stresses in coconut.

5. Conclusions

ARFs have been associated with a repertoire of plant growth and developmental processes and stress-adaptation responses. In this study, a total of 20 *CnARF*s were categorized by genome mining of a dwarf coconut cultivar. Insights on the evolutionary characteristics of CnARFs could be elucidated via identification of conserved motifs, intron-exon structure and phylogenetic analysis of palm ARFs. Expression profiling of CnARFs, in response to the imposition of osmotic and temperature stresses and growth regulators, provided valuable cues on the transcriptional regulation and involvement of specific CnARFs in coconut auxin-signaling cascades. Additionally, protein-protein interaction analysis elucidated the relationships of CnARFs and its interacting partners, at the transcriptional level. The results obtained present novel perceptions into the organization of coconut ARF family, and lead the way for the breeding of climate-smart coconuts.

Compliance with ethical requirements

This study did not involve human or animal subjects.

Author contributions

RMK, PKD, and SCKV conceived the idea and designed the experiments. RMK, SCKV, RSV, MKS, GKP carried out the experiments and generated the data. RMK, SCKV, RSV, MKS, GKP, PG, and PKD analyzed the data; RMK and SCKV prepared the manuscript with contribution from RSV, MKS, GKP, PG, and PKD. All authors read the MS and approved the submission.

Funding

This work was supported by funding from the Indian Council of Agricultural Research (ICAR-CPCRI Project No. 1000761030). Research in PKD lab is supported by ICAR-NPFGGM (formerly NPTC) project.

Declaration of Competing Interest

The authors declare that the research was conducted in the absence of any commercial or financial relationships that could be construed as a potential conflict of interest.

Appendix A. Supplementary data

Supplementary data to this article can be found online at https://doi.org/10.1016/j.plgene.2021.100344.

References

Arunachalam, V., Rajesh, M.K., 2008. Breeding of coconut palm (*Cocos nucifera* L.). CAB Rev. 3 (053), 1–12. https://doi.org/10.1079/PAVSNNR20083053.
Arunachalam, V., Rajesh, M.K., 2017. Coconut genetic diversity, conservation and utilization. In: Ahuja, M.R., Jain, M. (Eds.), Biodiversity and Conservation of Woody Plants. Springer, Cham, pp. 3–36. https://doi.org/10.1007/978-3-319-66426-2_1.
Aya, K., Hobo, T., Sato-Izawa, K., Ueguchi-Tanaka, M., Kitano, H., Matsuoka, M., 2014. A novel AP2-type transcription factor, SMALLORGANSIZE1, controls organ size downstream of an auxin signalling pathway. Plant Cell Physiol. 55, 897–912. https://doi.org/10.1093/pcp/pcu023.
Bandupriya, H.D., Dunwell, J.M., 2015. Transcriptome analysis for discovering candidate genes involve in embryogenesis in coconut (*Cocos nucifera* L.) through 454 pyro sequencing. J. Natl. Sci. Foun. Sri. 43, 319–336. https://doi.org/10.4038/jnsfsr.v43i4.7967.
Barrett, C.F., McKain, M.R., Sinn, B.T., Ge, X.J., Zhang, Y., Antonelli, A., Bacon, C.D., 2019. Ancient polyploidy and genome evolution in palms. Genome Biol. Evol. 11, 1501–1511. https://doi.org/10.1093/gbe/evz092.
Belin, C., Megies, C., Hauserová, E., Lopez-Molina, L., 2009. Abscisic acid represses growth of the *Arabidopsis embryonic* axis after germination by enhancing auxin signaling. Plant Cell 21 (8), 2253–2268. https://doi.org/10.1105/tpc.109.067702.
Boer, D.R., Freire-Rios, A., van den Berg, W.A., Saaki, T., Manfield, I.W., Kepinski, S., López-Vidrieo, I., Franco-Zorrilla, J.M., de Vries, S.C., Solano, R., Weijers, D., 2014. Structural basis for DNA binding specificity by the auxin-dependent ARF transcription factors. Cell 156, 577–589.
Chandler, J.W., 2016. Auxin response factors. Plant Cell Environ. 39, 1014–1028.
Dharmasiri, N., Dharmasiri, S., Estelle, M., 2005. The F-box protein TIR1 is an auxin receptor. Nature 435, 441–445.
Di, D.-W., Zhang, C., Luo, P., An, C.-W., Guo, G.Q., 2016. The biosynthesis of auxin: how many paths truly lead to IAA? Plant Growth Regul. 78 (3), 275–285. https://doi.org/10.1007/s10725-015-0103-5.
Die, J.V., Gil, J., Millan, T., 2018. Genome-wide identification of the auxin response factor gene family in *Cicer arietinum*. BMC Genomics 19, 301. https://doi.org/10.1186/s12864-018-4695-9.
Du, H., Wu, N., Fu, J., Wang, S., Li, X., Xiao, J., Xiong, L., 2012. A GH3 family member, OsGH3-2, modulates auxin and abscisic acid levels and differentially affects drought and cold tolerance in rice. J. Exp. Bot. 63, 6467–6480. https://doi.org/10.1093/jxb/ers300.
Du, H., Liu, H., Xiong, L., 2013. Endogenous auxin and jasmonic acid levels are differentially modulated by abiotic stresses in rice. Front. Plant Sci. 4, 397.
Eeuwens, C.J., 1976. Mineral requirements for growth and callus initiation of tissue explants excised from mature coconut palms (*Cocos nucifera*) and cultured *in vitro*. Physiol. Plant. 36, 23–28. https://doi.org/10.1111/j.1399-3054.1976.tb05022.x.
FAO, 2021. FAOSTAT. Food and Agriculture Organization. http://www.fao.org/faostat/en/#data/QC. (Accessed 28 May 2021).
Feher, A., 2015. Somatic embryogenesis—stress-induced remodeling of plant cell fate. Biochim.Biophys.Acta 1849, 385–402.
Gangaraj, K.P., Rajesh, M.K., 2020. Dataset of dual RNA-sequencing of *Phytophthora palmivora* infecting coconut (*Cocos nucifera* L.). Data Brief 30, 105455.
Gidhi, A., Kumar, M., Mukhopadhyay, K., 2020. The auxin response factor gene family in wheat (*Triticum aestivum* L.): genome-wide identification, characterization and expression analyses in response to leaf rust. South Afr. J. Bot. 140, 312–325.
Goetz, M., Vivian-Smith, A., Johnson, S.D., Koltunow, A.M., 2006. AUXIN RESPONSE FACTOR8 is a negative regulator of fruit initiation in *Arabidopsis*. Plant Cell 18, 1873–1886. https://doi.org/10.1105/tpc.105.037192.
Guilfoyle, T.J., 2015. The PB1 domain in auxin response factor and aux/IAA proteins: a versatile protein interaction module in the auxin response. Plant Cell 27, 33–43. https://doi.org/10.1105/tpc.114.132753.
Guilfoyle, T.J., Hagen, G., 2007. Auxin response factors. Curr.Opin. Plant Biol. 10, 453–460. https://doi.org/10.1016/j.pbi.2007.08.014.
Hagen, G., Guilfoyle, T., 2002. Auxin-responsive gene expression: genes, promoters and regulatory factors. Plant Mol. Biol. 49, 373–385. https://doi.org/10.1023/A:1015207114117.
Hardtke, C.S., Berleth, T., 1998. The *Arabidopsis* gene MONOPTEROS encodes a transcription factor mediating embryo axis formation and vascular development. EMBO J. 17, 1405–1411. https://doi.org/10.1093/emboj/17.5.1405.
Harper, R.M., Stowe-Evans, E.L., Luesse, D.R., Muto, H., Tatematsu, K., Watahiki, M.K., Yamamoto, K., Liscum, E., 2000. The NPH4 locus encodes the auxin response factor ARF7, a conditional regulator of differential growth in aerial *Arabidopsis* tissue. Plant Cell 12, 757–770. https://doi.org/10.1105/tpc.12.5.757.

Hu, W., Zuo, J., Hou, X., Yan, Y., Wei, Y., Liu, J., Li, M., Xu, B., Jin, Z., 2015. The auxin response factor gene family in banana: genome-wide identification and expression analyses during development, ripening, and abiotic stress. Front. Plant Sci. 6, 742. https://doi.org/10.3389/fpls.2015.00742.

Jin, L., Yarra, R., Zhou, L., Cao, H., 2021. The auxin response factor (ARF) gene family in oil palm (*Elaeis guineensis* Jacq.): genome-wide identification and their expression profiling under abiotic stresses. Protoplasma. https://doi.org/10.1007/s00709-021-01639-9.

Kalve, S., Sizani, B.L., Markakis, M.N., Helsmoortel, C., Vandeweyer, G., Laukens, K., Sommen, M., Naulaerts, S., Vissenberg, K., Prinsen, E., Beemster, G.T., 2020. Osmotic stress inhibits leaf growth of *Arabidopsis thaliana* by enhancing ARF-mediated auxin responses. New Phytol. 226, 1766–1780. https://doi.org/10.1111/nph.16490.

Kepinski, S., Leyser, O., 2005. The *Arabidopsis* F-box protein TIR1 is an auxin receptor. Nature 435, 446–451.

Kunkel, B.N., Johnson, J.M., 2021. Auxin plays multiple roles during plant–pathogen interactions. Cold Spring Harb. Perspect. Biol. https://doi.org/10.1101/cshperspect.a040022 p.a040022.

Li, S.B., Ou Yang, W.Z., Hou, X.J., Xie, L.L., Hu, C.G., Zhang, J.Z., 2015. Genome-wide identification, isolation and expression analysis of auxin response factor (ARF) gene family in sweet orange (*Citrus sinensis*). Front. Plant Sci. 6, 119. https://doi.org/10.3389/fpls.2015.00119.

Li, S.B., Xie, Z.Z., Hu, C.G., Zhang, J.Z., 2016. A review of auxin response factors (ARFs) in plants. Front. Plant Sci. 7, 47. https://doi.org/10.3389/fpls.2016.00047.

Liscum, E., Reed, J., 2002. Genetics of *Aux/IAA* and *ARF* action in plant growth and development. Plant Mol. Biol. 49, 387–400. https://doi.org/10.1023/A:1015255030047.

Liu, N., Dong, L., Deng, X., Liu, D., Liu, Y., Li, M., Hu, Y., Yan, Y., 2018a. Genome-wide identification, molecular evolution, and expression analysis of auxin response factor (ARF) gene family in *Brachypodium distachyon* L. BMC Plant Biol. 18 (1), 1–15. https://doi.org/10.1186/s12870-018-1559-z.

Liu, M., Ma, Z., Wang, A., Zheng, T., Huang, L., Sun, W., Zhang, Y., Jin, W., Zhan, J., Cai, Y., Tang, Y., 2018b. Genome-wide investigation of the auxin response factor gene family in Tartary buckwheat (*Fagopyrumum tataricum*). Int. J. Mol. Sci. 19, 3526. https://doi.org/10.3390/ijms19113526.

Livak, K.J., Schmittgen, T.D., 2001. Analysis of relative gene expression data using real-time quantitative PCR and the 2(−Delta DeltaC(T)) method. Methods 25, 402–408. https://doi.org/10.1006/meth.2001.1262.

Matilla, A.J., 2020. Auxin: hormonal signal required for seed development and dormancy. Plants 9 (6), 705. https://doi.org/10.3390/plants9060705.

Nagpal, P., Ellis, C.M., Weber, H., Ploense, S.E., Barkawi, L.S., Guilfoyle, T.J., Hagen, G., Alonso, J.M., Cohen, J.D., Farmer, E.E., Ecker, J.R., 2005. Auxin response factors ARF6 and ARF8 promote jasmonic acid production and flower maturation. Development 132 (18), 4107–4118.

Narise, T., Kobayashi, K., Baba, S., Shimojima, M., Masuda, S., Fukaki, H., Ohta, H., 2010. Involvement of auxin signalling mediated by IAA14 and ARF7/19 in membrane lipid remodelling during phosphate starvation. Plant Mol. Biol. 72, 533–544. https://doi.org/10.1007/s11103-009-9589-4.

Nejat, N., Cahill, D.M., Vadamalai, G., Ziemann, M., Rookes, J., Naderali, N., 2015. Transcriptomics-based analysis using RNA-Seq of the coconut (*Cocos nucifera*) leaf in response to yellow decline phytoplasma infection. Mol. Gen. Genomics. 290, 1899–1910. https://doi.org/10.1007/s00438-015-1046-2.

Nishimura, T., Wada, T., Yamamoto, K.T., Okada, K., 2005. The *Arabidopsis* STV1 protein, responsible for translation re-initiation, is required for auxin-mediated gynoecium patterning. Plant Cell 17, 2940–2953. https://doi.org/10.1105/tpc.105.036533.

Niu, J., Bi, Q., Deng, S., Chen, H., Yu, H., Wang, L., Lin, S., 2018. Identification of AUXIN RESPONSE FACTOR gene family from *Prunussibirica* and its expression analysis during mesocarp and kernel development. BMC Plant Biol. 18, 1–11. https://doi.org/10.1186/s12870-017-1220-2.

Ooi, S.E., Choo, C.N., Ishak, Z., Ong-Abdullah, M., 2012. A candidate auxin-responsive expression marker gene, *EgIAA9*, for somatic embryogenesis in oil palm (*Elaeis guineensis*Jacq.). Plant Cell Tissue Organ Cult. 110, 201–212. https://doi.org/10.1007/s11240-012-0143-8.

Okushima, Y., Overvoorde, P.J., Arima, K., Alonso, J.M., Chan, A., Chang, C., Ecker, J.R., Hughes, B., Lui, A., Nguyen, D., Onodera, C., 2005. Functional genomic analysis of the AUXIN RESPONSE FACTOR gene family members in *Arabidopsis thaliana*: unique and overlapping functions of ARF7 and ARF19. Plant Cell 17, 444–463. https://doi.org/10.1105/tpc.104.028316.

Park, C.M., 2007. Auxin homeostasis in plant stress adaptation response. Plant Signal. Behav. 2 (4), 306–307. https://doi.org/10.4161/psb.2.4.4069.

Park, J.E., Park, J.Y., Kim, Y.S., Staswick, P.E., Jeon, J., Yun, J., Kim, S.Y., Kim, J., Lee, Y. H., Park, C.M., 2007. GH3-mediated auxin homeostasis links growth regulation with stress adaptation response in *Arabidopsis*. J. Biol. Chem. 282, 10036–10046. https://doi.org/10.1074/jbc.M610524200.

Pérez-Rodríguez, P., Riaño-Pachón, D.M., Corrêa, L.G., Rensing, S.A., Kersten, B., Mueller-Roeber, B., 2010. Pln TFDB: updated content and new features of the plant transcription factor database. Nucleic Acids Res. 38, D822–D827. https://doi.org/10.1093/nar/gkp805.

Qi, Y., Wang, S., Shen, C., Zhang, S., Chen, Y., Xu, Y., Liu, Y., Wu, Y., Jiang, D., 2012. OsARF12, a transcription activator on auxin response gene, regulates root elongation and affects iron accumulation in rice (*Oryza sativa*). New Phytol. 193, 109–120. https://doi.org/10.1111/j.1469-8137.2011.03910.x.

Rachana, K.E., Rajesh, M.K., 2019. Selection and validation of reference genes for gene expression normalization in coconut (*Cocos nucifera* L.) under biotic stress and hormone stimuli. Plant Gene 19, 100184. https://doi.org/10.1016/j.plgene.2019.100184.

Raghavendra, A.S., Gonugunta, V.K., Christmann, A., Grill, E., 2010. ABA perception and signalling. Trends Plant Sci. 15 (7), 395–401. https://doi.org/10.1016/j.tplants.2010.04.006.

Rajesh, M.K., Rachana, K.E., Naganeeswaran, S., Shafeeq, R., Thomas, R.J., Shareefa, M., Merin, B., Karun, A., 2015. Identification of expressed resistance gene analog sequences in coconut leaf transcriptome and their evolutionary analysis. Turk. J. Agric. For. 39, 489–502. https://doi.org/10.3906/tar-1409-75.

Rajesh, M.K., Fayas, T.P., Naganeeswaran, S., Rachana, K.E., Bhavyashree, U., Sajini, K. K., Karun, A., 2016. *De novo* assembly and characterization of global transcriptome of coconut palm (*Cocos nucifera* L.) embryogenic calli using Illumina paired-end sequencing. Protoplasma 253, 913–928. https://doi.org/10.1007/s00709-015-0856-8.

Rajesh, M.K., Rachana, K.E., Kulkarni, K., Sahu, B.B., Thomas, R.J., Karun, A., 2018. Comparative transcriptome profiling of healthy and diseased Chowghat green dwarf coconut palms from root (wilt) disease hot spots. Eur. J. Plant Pathol. 151, 173–193. https://doi.org/10.1007/s10658-017-1365-8.

Rajesh, M.K., Chowdappa, P., Behera, S.K., Kasaragod, S., Gangaraj, K.P., Kotimoole, C. N., Nekrakalaya, B., Mohanty, V., Sampgod, R.B., Banerjee, G., Das, A.J., 2020. Assembly and annotation of the nuclear and organellar genomes of a dwarf coconut (Chowghat green dwarf) possessing enhanced disease resistance. OMICS: J. Integr. Biol. 24 (12), 726–742.

Ramesh, S.V., Arunachalam, V., Rajesh, M.K., 2020. Genomic designing of climate-smart coconut. In: Kole, C. (Ed.), Genomic Designing of Climate-Smart Fruit Crops. Springer, Cham, pp. 3–36. https://doi.org/10.1007/978-3-319-97946-5_6.

Rock, C.D., Sun, X., 2005. Crosstalk between ABA and auxin signaling pathways in roots of *Arabidopsis thaliana* (L.) Heynh. Planta 222 (1), 98–106. https://doi.org/10.1007/s00425-005-1521-9.

Roosjen, M., Paque, S., Weijers, D., 2018. Auxin response factors: output control in auxin biology. J. Exp. Bot. 69 (2), 179–188.

Sabana, A.A., Rajesh, M.K., Antony, G., 2020. Dynamic changes in the expression pattern of miRNAs and associated target genes during coconut somatic embryogenesis. Planta 251, 1–18. https://doi.org/10.1007/s00425-020-03368-4.

Saitou, N., Nei, M., 1987. The neighbor-joining method: a new method for reconstructing phylogenetic trees. Mol. Biol. Evol. 4, 406–425. https://doi.org/10.1093/oxfordjournals.molbev.a040454.

Shen, C., Yue, R., Sun, T., Zhang, L., Xu, L., Tie, S., Wang, H., Yang, Y., 2015. Genome-wide identification and expression analysis of auxin response factor gene family in *Medicago truncatula*. Front. Plant Sci. 6, 73. https://doi.org/10.3389/fpls.2015.00073.

Song, S., Hao, L., Zhao, P., Xu, Y., Zhong, N., Zhang, H., Liu, N., 2019. Genome-wide identification, expression profiling and evolutionary analysis of auxin response factor gene family in potato (*Solanum tuberosum* group phureja). Sci. Rep. 9 (1), 1–13.

Szemenyei, H., Hannon, M., Long, J.A., 2008. TOPLESS mediates auxin dependent transcriptional repression during *Arabidopsis* embryogenesis. Science 319, 1384–1386. https://doi.org/10.1126/science.1151461.

Tang, Y., Bao, X., Liu, K., Wang, J., Zhang, J., Feng, Y., Wang, Y., Lin, L., Feng, J., Li, C., 2018. Genome-wide identification and expression profiling of the auxin response factor (ARF) gene family in physic nut. PLoS One 13 (8), e0201024. https://doi.org/10.1371/journal.pone.0201024.

Tiwari, S.B., Hagen, G., Guilfoyle, T., 2003. The roles of auxin response factor domains in auxin-responsive transcription. Plant Cell 15, 533–543.

Tombuloglu, H., 2019. Genome-wide analysis of the auxin response factors (ARF) gene family in barley (*Hordeum vulgare* L.). J. Plant Biochem. Biotechnol. 28 (1), 14–24.

Van Ha, C., Le, D.T., Nishiyama, R., Watanabe, Y.A., Sulieman, S., Tran, U.T., Mochida, K., Van Dong, N., Yamaguchi-Shinozaki, K., Shinozaki, K., Tran, L.S., 2013. The auxin response factor transcription factor family in soybean: genome-wide identification and expression analyses during development and water stress. DNA Res. 20, 511–524. https://doi.org/10.1093/dnares/dst027.

Wang, D., Pei, K., Fu, Y., Sun, Z., Li, S., Liu, H., Tang, K., Han, B., Tao, Y., 2007. Genome-wide analysis of the auxin response factors (ARF) gene family in rice (*Oryza sativa*). Gene 394, 13–24. https://doi.org/10.1016/j.gene.2007.01.006.

Weijers, D., Wagner, D., 2016. Transcriptional responses to the auxin hormone. Annu. Rev. Plant Biol. 67, 539–574.

Wen, J., Guo, P., Ke, Y., Liu, M., Li, P., Wu, Y., Ran, F., Wang, M., Li, J., Du, H., 2019. The auxin response factor gene family in allopolyploid *Brassica napus*. PLoS One 14, e0214885. https://doi.org/10.1371/journal.pone.0214885.

Wu, M., Wu, J., Gan, Y., 2020. The new insight of auxin functions: transition from seed dormancy to germination and floral opening in plants. Plant Growth Regul. 91 (2), 169–174.

Xia, W., Liu, Z., Yang, Y., Xiao, Y., Mason, A.S., Zhao, S., Ma, Z., 2014. Selection of reference genes for quantitative real-time PCR in *Cocos nucifera* during abiotic stress. Botany 92 (3), 179–186.

Xing, H., Pudake, R.N., Guo, G., Xing, G., Hu, Z., Zhang, Y., Sun, Q., Ni, Z., 2011. Genome-wide identification and expression profiling of auxin response factor (ARF) gene family in maize. BMC Genomics 12, 178. https://doi.org/10.1186/1471-2164-12-178.

Xu, Y.X., Mao, J., Chen, W., Qian, T.T., Liu, S.C., Hao, W.J., Li, C.F., Chen, L., 2016. Identification and expression profiling of the auxin response factors (ARFs) in the tea plant (*Camellia sinensis* (L.) O. Kuntze) under various abiotic stresses. Plant Physiol. Biochem. 98, 46–56. https://doi.org/10.1016/j.plaphy.2015.11.014.

Yu, H., Soler, M., Mila, I., San Clemente, H., Savelli, B., Dunand, C., Paiva, J.A., Myburg, A.A., Bouzayen, M., Grima-Pettenati, J., Cassan-Wang, H., 2014. Genome-wide characterization and expression profiling of the AUXIN RESPONSE FACTOR

(ARF) gene family in *Eucalyptus grandis*. PLoS One 9, e108906. https://doi.org/10.1371/journal.pone.0108906.

Zhang, H., Jin, J., Tang, L., Zhao, Y., Gu, X., Gao, G., Luo, J., 2011. Plant TFDB 2.0: update and improvement of the comprehensive plant transcription factor database. Nucleic Acids Res. 39, D1114–D1117. https://doi.org/10.1093/nar/gkq1141.

Zhang, Y., Zeng, Z., Chen, C., Li, C., Xia, R., Li, J., 2019. Genome-wide characterization of the auxin response factor (ARF) gene family of litchi (*Litchi chinensis*Sonn.): phylogenetic analysis, miRNA regulation and expression changes during fruit abscission. Peer J. 7, e6677 https://doi.org/10.7717/peerj.6677.

Zouine, M., Fu, Y., Chateigner-Boutin, A.L., Mila, I., Frasse, P., Wang, H., Audran, C., Roustan, J.P., Bouzayen, M., 2014. Characterization of the tomato ARF gene family uncovers a multi-levels post-transcriptional regulation including alternative splicing. PLoS One 9 (1), e84203. https://doi.org/10.1371/journal.pone.0084203.